Inelastic Quantum Transport and Peierls-Like Mechanism in Carbon Nanotubes

Luis E. F. Foa Torres[1,2] and Stephan Roche[1]
[1]CEA/DSM/DRFMC/SPSMS/GT, 17 avenue des Martyrs, 38054 Grenoble, France
[2]CEA/DRT/LETI/DIHS/LMNO, 17 avenue des Martyrs, 38054 Grenoble, France
(Received 12 May 2006; published 18 August 2006)

We report on a theoretical study of inelastic quantum transport in $(3m, 0)$ carbon nanotubes. By using a many-body description of the electron-phonon interaction in Fock space, a novel mechanism involving optical phonon emission (absorption) is shown to induce an unprecedented energy-gap opening at half the phonon energy, $\hbar\omega_0/2$, above (below) the charge neutrality point. This mechanism, which is prevented by Pauli blocking at low bias voltages, is activated at bias voltages on the order of $\hbar\omega_0$.

DOI: 10.1103/PhysRevLett.97.076804 PACS numbers: 73.63.Fg, 05.60.Gg, 72.10.Di, 73.23.−b

Since their discovery, carbon nanotubes (CNTs) have attracted much attention due to their outstanding mechanical and electrical properties [1]. Depending on their helicity, CNTs exhibit either semiconducting or metallic behavior, and, for low resistance contacts, ballistic transport is observed in the low bias regime. At higher bias, several experimental works report on current saturation, attributed to inelastic (interband) backscattering by optical phonons [2]. Electron-phonon (e-ph) interaction thus severely limits the exceptional properties of CNTs as ballistic conductors. Aimed to the explanation of the experimental data [2–4], several theoretical studies of electronic transport in CNTs in the presence of e-ph interaction were performed [5–10]. They include simulations based on the Boltzmann equation [5,10], the Fermi golden rule [6], and the use of a diagonal self-consistent Born approximation [7]. Besides, in order to explain the quantitative disagreement between theoretical and experimental estimations of inelastic mean free paths, a hot phonons scenario was recently proposed [6].

On the other hand, electron-phonon coupling in low-dimensional systems can lead to more subtle effects and important corrections to both phonon and electronic band structures. Fundamental examples are the Kohn anomaly [11] and the Peierls transition [12,13]. Connected to the latter, and by using density functional theory, Dubay and co-workers found a softening of the mode with A_1 symmetry in metallic CNTs, not sufficient, however, to produce a static lattice distortion [14]. Notwithstanding, as explored within the linear response regime, the corresponding phonon-induced (time-dependent) electronic band structure changes result in strong modifications of the Kubo conductance [9]. This points towards the importance for a quantum mechanical treatment of inelastic transport whenever high energy (optical) modes are activated.

In this Letter, by using a full quantum description of the joined processes of tunneling and phonon-assisted transport, the coupling between electrons and optical $A_1(L)$ phonons in $(N = 3m, 0)$ zigzag tubes is shown to result in an energy-gap opening at $\hbar\omega_0/2$ above (below) the charge neutrality point (CNP), owing to phonon emission (absorption). This novel many-body mechanism is activated when driving the system out of equilibrium.

For simplicity, we consider an infinite CNT and allow the electrons to interact with phonons only in a central part of length L. The Hamiltonian of the system is written as a sum of an electronic part, a phonon part, and the e-ph interaction term. The electronic part is described by an effective π-orbitals model $H_e = -\gamma_0 \sum_{\langle i,j \rangle} [c_i^+ c_j + \text{H.c.}]$, where c_i^+ and c_i are the creation and annihilation operators for electrons at site i, respectively, and $\gamma_0 = 2.77$ eV is the transfer integral restricted to nearest neighbor π orbitals [1]. The phonon term is given by $H_{\text{ph}} = \hbar\omega_0 b^+ b$, with b^+ and b the phonon operators. The remaining contribution is given by a Su-Schreiffer-Heeger Hamiltonian [15], describing the e-ph coupling to a nonlocal vibrational eigenmode. This is found by assuming a phonon modulation of the hopping matrix elements [15,16], keeping only the linear corrections to the atomic displacements from equilibrium, i.e., $\gamma_{i,j} = \gamma_0 + \alpha \hat{\delta}_{i,j} \cdot \delta\vec{Q}_{i,j}$, where $\hat{\delta}_{i,j}$ is a unit vector in the bond direction, $\delta\vec{Q}_{i,j}$ is the relative displacement of the neighboring carbon atoms, and α is the e-ph coupling strength defined as the derivative of γ_0 with respect to the change in the bond length. Further quantization of the atomic displacements gives the e-ph interaction term:

$$H_{e\text{-ph}} = \sum_{\langle i,j \rangle_{\text{vib}}} [\gamma_{i,j}^{e\text{-ph}} c_i^+ c_j (b^+ + b) + \text{H.c.}], \qquad (1)$$

where the e-ph matrix elements can be written as $\gamma_{i,j}^{e\text{-ph}} = \alpha\sqrt{\hbar/(2m\omega_0)}\hat{\delta}_{i,j} \cdot (\hat{e}_i - \hat{e}_j)$; $\hat{e}_i$ is the phonon mode eigenvector which gives the atomic displacements. The summation in the right-hand side corresponds to nearest neighbors within the vibrating region of the CNT. For the phonon mode considered here $[A_1(L)]$, A- and B-type atoms move out of phase in the direction parallel to the tube axis (see scheme in Fig. 1).

To compute inelastic quantum transport, we use the approach introduced in Refs. [17,18], which has been applied to a variety of problems including vibration-

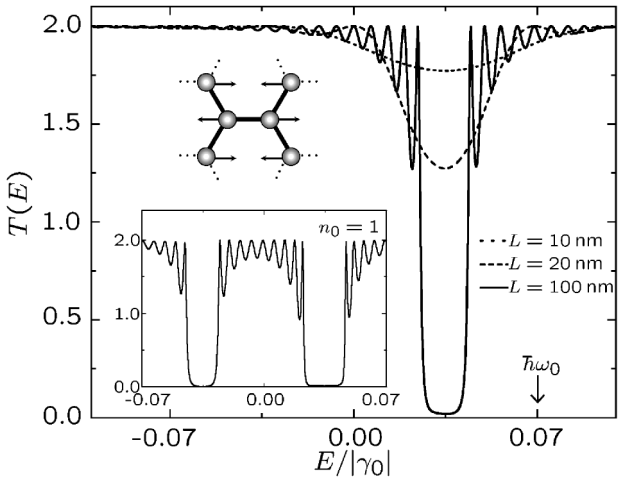

FIG. 1. Total transmission probability as a function of the energy of the incident electrons for $n_0 = 0$. Inset: Same information for $n_0 = 1$. The results correspond to a (24, 0) tube where interaction with an $A_1(L)$ mode inducing displacements along the axis direction (drawing) is included. Note that a total energy $\varepsilon = \hbar\omega_0/2$ corresponds to an electronic kinetic energy $E = \hbar\omega_0/2$ for $n = 0$ and $-\hbar\omega_0/2$ for $n = 1$.

assisted tunneling in STM experiments [19], transport through molecules [20,21], and resonant tunneling in double barrier heterostructures [22]. This scheme allows an exact nonperturbative treatment of the problem of one electron transport in the presence of e-ph interaction. This is achieved by an exact mapping of the many-body problem into a single particle problem in a higher dimensional space (the e-ph Fock space), each considered phonon mode adding one extra dimension to the problem. The key idea behind this approach can be visualized after rewriting the interacting Hamiltonian in an appropriate basis for the e-ph Fock space (one electron plus phonons). In this equivalent multichannel one-body problem, the asymptotic states (in the noninteracting leads) include both the electronic and the vibrational degrees of freedom and the total energy is fully conserved. When considering a single phonon mode, these asymptotic channels can be labeled by using two indexes: (X, n), $X = L, R$ being the index associated to the corresponding electrode (left or right) and n the number of phonon excitations in the system. Accordingly, the transmission $T_{(X,n)\to(Y,m)}$ and reflection probabilities $R_{(X,n)\to(Y,m)}$ between the different channels are computed by using standard Green's functions techniques [22]. Using these probabilities as inputs, the nonequilibrium electron distributions in the leads (at finite temperature and bias voltage) are evaluated self-consistently using the procedure developed in Ref. [21]. The electronic current through the device can be obtained from these self-consistent distributions, which take into account the Pauli exclusion principle for the different competing processes.

Let us first explicitly establish how the Fock states are connected by the Hamiltonian and simplify the problem by using a mode decomposition. The matrix elements of the e-ph Hamiltonian are essentially given by the projection of the bond direction on the relative displacements of the atoms from their equilibrium positions $\hat{\delta}_{i,j} \cdot (\hat{e}_i - \hat{e}_j)$. It can be easily proven that the e-ph matrix elements $\gamma_{i,j}^{e\text{-ph}}$ have values $\gamma_0^{e\text{-ph}} = -2\alpha\sqrt{\hbar/(2m\omega_0)}$ for bonds (i, j) that are parallel to the tube axis and $-\gamma_0^{e\text{-ph}}\cos(\pi/3)$ for bonds (i, j) that are tilted with respect to the tube axis.

For the phonon mode considered here, instead of solving the Hamiltonian in real space, one uses a mode space approach [7,23]. The idea is to resort to a unitary transformation that diagonalizes the electronic Hamiltonian for each layer perpendicular to the tube axis. The resulting eigenstates will correspond to different circumferential modes that can be used to build an alternative basis for the description of transport through the nanotube. In the absence of static disorder, the electronic Hamiltonian H_e does not couple the different modes, and the different subbands correspond to linear chains with alternating hoppings γ_0 and $\gamma_q = 2\gamma_0\cos(q\pi/N)$ $(q = 0, 1, \ldots, N-1)$ with dispersion relations: $\varepsilon^{(0)}(k) = \pm\sqrt{\gamma_0^2 + \gamma_q^2 + 2\gamma_0\gamma_q\cos(3ka_{cc}/2)}$. When N is an integer multiple of 3, the metallic subbands correspond to $q = N/3$, $2N/3$. Furthermore, since the e-ph Hamiltonian $H_{e\text{-ph}}$ does not couple different circumferential modes, one is left with N independent problems. Each of them corresponds to a one-dimensional mode space lattice that, when coupled to phonons, gives a two-dimensional problem in Fock space.

In Fig. 1, one reports the total transmission probability $T(E) = \sum_n T_{(L,n_0)\to(R,n)}(E)$ as a function of the incident's electron energy E, when there are initially no phonon excitations in the system, $n_0 = 0$. All the energies are expressed in units of γ_0, the value of $\hbar\omega_0$ is taken as $0.07\gamma_0$ [14], and $\alpha = \alpha_0 \simeq 7$ eV/Å is estimated from Ref. [24]. For short nanotube lengths ($L = 10$ nm), the main feature is the occurrence of a transmission dip centered at $E = \hbar\omega_0/2$ above the CNP that progressively deepens with CNT length, to reach a full gap at $L = 100$ nm, and with a width of approximately $3\gamma_0^{e\text{-ph}}$. Apart from this fundamental gap, the effect of e-ph interaction remains small. The transmission remains mostly elastic in all of the energy range shown in the plot. However, the reduction of the transmission probability in the gap region corresponds to a complementary increase in the inelastic backscattering by phonon emission.

Figure 1 (inset) shows the transmission probability in the situation where one phonon is already available for scattering before any additional charge enters into the sample. In this case, in addition to the expected enlargement of the gap at $E = \hbar\omega_0/2$ by a factor $\sqrt{2}$ due to stimulated phonon emission, another gap develops at $E = -\hbar\omega_0/2$. This transmission gap is complemented by an increase in the inelastic backscattering by phonon absorption.

To provide a clear physical picture of such phenomena, let us consider that the sample, i.e., the region where the

e-ph interaction is allowed, extends to infinity. The Fock space for the coupled e-ph system can then be expanded in terms of the basis states $\{|l_q, n\rangle = |l_q\rangle \otimes |n\rangle\}$, where $|l_q\rangle$ is the qth circumferential mode localized in the lth layer and $|n\rangle$ corresponds to the state with n phonons in the system. Close to the CNP, only two circumferential modes participate in conduction ($q = N/3,\ 2N/3$). The e-ph Hamiltonian for one of those modes is represented in Fig. 2 (upper inset). Alternatively, the Fock space for an individual mode can be expanded by using plane waves instead of localized states for the electronic part. This leads to basis states of the form $|k, n\rangle = |k\rangle \otimes |n\rangle$, where $|k\rangle$ is a plane wave in mode space with wave vector k along the axis direction.

Let us consider the circumferential mode with $q = N/3$, though a similar reasoning holds for $q = 2N/3$. In absence of e-ph coupling, one gets disconnected chains associated to the different values of n, each one with hoppings $\gamma_q = \gamma_0$ and unperturbed dispersion relations $\varepsilon_n^{(0)} = \varepsilon_n^{(0)}(k)$ (see Fig. 2). Of particular interest are the states $|k_+ = \pi/2a + |\delta k|, 0\rangle$ and $|k_+ - K, 1\rangle$ (black circles), where $a = 3a_{cc}/4$ and $K = \pi/a$. They have the same total energy $\varepsilon_0^{(0)}(k_+) = \varepsilon_1^{(0)}(k_+ - K) = \hbar\omega_0/2$. When the e-ph interaction is switched on, the lattice period of the many-body Hamiltonian is doubled because of the spatial periodicy of $H_{e\text{-ph}}$. The new lattice vector is $K = \pi/a$ instead of $2\pi/a$. *The mentioned Fock states are now mixed by* $H_{e\text{-ph}}$, i.e., $\langle k_+ - K, 1|H_{e\text{-ph}}|k_+, 0\rangle = \Delta\gamma^{e\text{-ph}} \equiv (3/2)\gamma_0^{e\text{-ph}} \neq 0$ [25]. The degeneracy is thus lifted, giving rise to the opening of an energy gap in $\varepsilon_0(k)$ and $\varepsilon_1(k)$ of width $2|\Delta\gamma^{e\text{-ph}}|$ around $\varepsilon = \hbar\omega_0/2$ (right inset in Fig. 2). Accordingly, an incoming electron with a wave vector k in the Fock state $|k, n\rangle$ will contain, as k approaches k_+ (or $k_+ - K$), an increasing admixture of $|k - K, n + 1\rangle$ (or $|k + K, n - 1\rangle$) leading to a Bragg-type inelastic scattering. This mechanism is due to a modification of the translational symmetry of the system driven by the e-ph interaction, with no static distortion of the lattice. A similar effect holds for the other states marked as symbols of the same kind in Fig. 2 and for the subband with $q = 2N/3$. This results in the transmission gaps shown in Fig. 1 which are in quantitative agreement with the prior analysis.

Figure 3 shows the transmission minimum at the center of the phonon emission gap $T(E = \hbar\omega_0/2)$ as a function of the nanotube length. Different curves correspond to different values of the parameter α entering into the e-ph matrix elements $\gamma_{i,j}^{e\text{-ph}}$. From a simple argument, one can predict the existence of a region where the transmission decays exponentially with the tube length (tunneling through the gap), i.e., $T \propto \exp(-L/\xi)$, with a decay length ξ that is inversely proportional to the energy gap $\Delta\gamma^{e\text{-ph}}$. Another interesting feature is the observed saturation for longer tubes. The saturation value T_{sat} as a function of α^2 (inset in Fig. 3) is associated to the small inelastic component of the transmission.

It should be noted that the opening of the transmission gap will be prevented by Pauli blocking at low bias voltage. In order to activate it, the system has to be driven out of equilibrium by applying a sufficiently high bias between the voltage probes. To explore the consequences of this phenomenon in the current-voltage characteristics, the effect of the bias voltage is introduced on H_e by modifying the on site energies of the π orbitals. The potential drop is assumed to be equally distributed at the two contacts. The

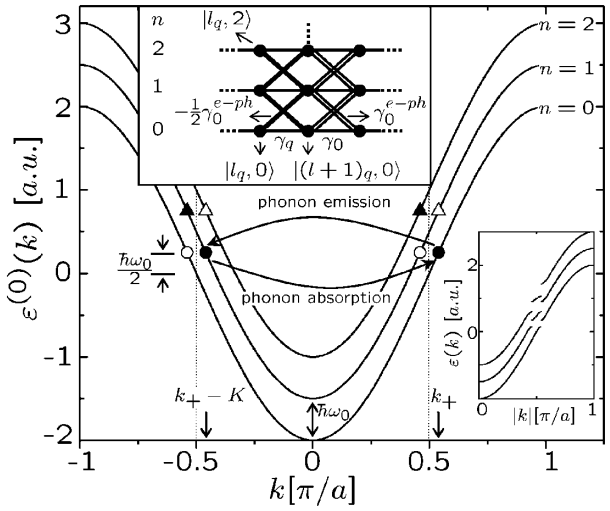

FIG. 2. Scheme for the unperturbed ($H_{e\text{-ph}} = 0$) dispersion relations corresponding to $n = 0, 1, 2$ for the mode $q = N/3$. The states marked with identical symbols correspond to degenerate states of the coupled e-ph system. These degeneracies are lifted by the e-ph interaction leading to the opening of energy gaps at $\hbar\omega_0/2$ above (below) the band center (see right inset). Upper inset: Representation of the many-body Hamiltonian in Fock space for a circumferential mode q (note the two-layer periodicity). Solid circles represent states in Fock space, while the lines are off-diagonal matrix elements.

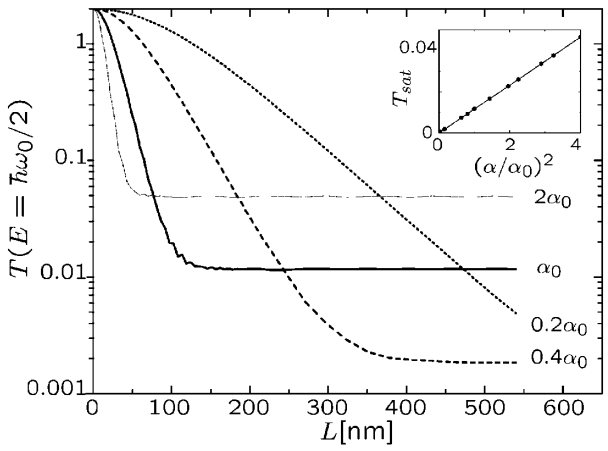

FIG. 3. Total transmission probability at $E = \hbar\omega_0/2$ as a function of the tube length for $n_0 = 0$; the other parameters are the same as in Fig. 1. The inset shows the saturation value of the total transmission as a function of α^2.

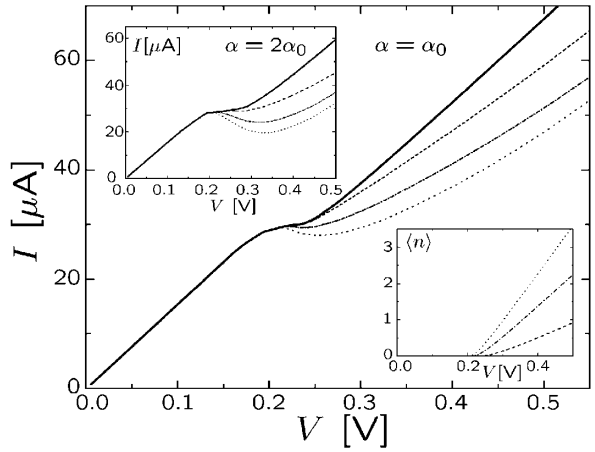

FIG. 4. Current vs bias voltage for a (24, 0) 150 nm long tube for $\alpha = \alpha_0$ (main frame) and $\alpha = 2\alpha_0$ (upper inset). Solid lines correspond to a fixed phonon population $n_0 = 0$. The dashed, dashed-dotted, and dotted lines correspond to the effective thermal distributions described in the text. The mean number of phonons corresponding to these curves are shown in the lower inset.

current-voltage curves calculated from this simple model for $\alpha = \alpha_0$ and $\alpha = 2\alpha_0$ and zero temperature are shown in Fig. 4 (solid lines in the main frame and inset, respectively). The main feature that results from the gap opening is the onset of a current plateau observed at $V \sim \hbar\omega_0$ whose width scales linearly with α. The subsequent linear increase in the current is due to the lack of other ingredients in our model such as electronic coupling with other phonon modes (such as those producing interband backscattering) or electrostatics effects. Motivated by recent studies that suggest the possible build up of a strong out-of-equilibrium phonon population at high bias voltages [3,6,10], a natural question is how such a scenario would modify our results. The answer might be provided by a self-consistent scheme to determine the out-of-equilibrium phonon population in the system, but this is beyond the scope of the present study. Instead, a thermalized phonon population with an effective temperature $k_B T_{\text{eff}}$ is assumed and $k_B T_{\text{eff}}(V)$ is supposed to increase linearly for $eV \geq \hbar\omega_0$ [3,6,10]. The dependence of the mean numbers of phonons with the bias voltage for different slopes in $k_B T_{\text{eff}}(V)$ (10, 20, and 30 kK/V) are shown in the lower inset. The corresponding currents for a 150 nm long tube are shown with dashed, dashed-dotted, and dotted lines for $\alpha = \alpha_0$ (Fig. 4) and $\alpha = 2\alpha_0$ (upper inset). A substantial decrease in the currents when the phonon population increases is observed. Furthermore, the dotted lines reveal the appearance of a region of negative differential resistance.

Semiconducting zigzag CNTs with a band gap smaller than $\hbar\omega_0$ are also found to display the phonon-induced transmission gap (not shown here). On the other hand, for CNTs other than zigzag, this phenomenon will be driven by the relevant optical phonon mode producing an instantaneous dimerization pattern of appropriate period in the axis direction. In contrast to the Peierls transition, where a mean field description is feasible [15], the proposed mechanism does not involve a static lattice distortion and is activated at high bias voltage.

This work was supported by the French Ministry of Research under Grant RTB: PostCMOS moléculaire 200mm.

[1] R. Saito, G. Dresselhaus, and M. S. Dresselhaus, *Physical Properties of Carbon Nanotubes* (Imperial College Press, London, 1998).
[2] Z. Yao, C. L. Kane, and C. Dekker, Phys. Rev. Lett. **84**, 2941 (2000).
[3] E. Pop *et al.*, Phys. Rev. Lett. **95**, 155505 (2005).
[4] A. Javey *et al.*, Phys. Rev. Lett. **92**, 106804 (2004).
[5] V. Perebeinos, J. Tersoff, and Ph. Avouris, Phys. Rev. Lett. **94**, 086802 (2005); M. A. Kuroda, A. Cangellaris, and J. P. Leburton, Phys. Rev. Lett. **95**, 266803 (2005).
[6] M. Lazzeri *et al.*, Phys. Rev. Lett. **95**, 236802 (2005).
[7] A. Svizhenko and M. P. Anantram, Phys. Rev. B **72**, 085430 (2005).
[8] M. Georghe *et al.*, Europhys. Lett. **71**, 438 (2005).
[9] S. Roche, J. Jiang, F. Triozon, and R. Saito, Phys. Rev. Lett. **95**, 076803 (2005).
[10] M. Lazzeri and F. Mauri, Phys. Rev. B **73**, 165419 (2006).
[11] S. Piscanec *et al.*, Phys. Rev. Lett. **93**, 185503 (2004).
[12] J. W. Mintmire, B. I. Dunlap, and C. T. White, Phys. Rev. Lett. **68**, 631 (1992); R. Saito, M. Fujita, G. Dresselhaus, and M. S. Dresselhaus, Phys. Rev. B **46**, 1804 (1992); K. Harigaya and M. Fujita, Phys. Rev. B **47**, 16 563 (1993).
[13] D. Connétable, G.-M. Rignanese, J.-C. Charlier, and X. Blase, Phys. Rev. Lett. **94**, 015503 (2005).
[14] O. Dubay, G. Kresse, and H. Kuzmany, Phys. Rev. Lett. **88**, 235506 (2002).
[15] W. P. Su, J. R. Schrieffer, and A. J. Heeger, Phys. Rev. Lett. **42**, 1698 (1979).
[16] G. D. Mahan, Phys. Rev. B **68**, 125409 (2003).
[17] E. V. Anda, S. S. Makler, H. M. Pastawski, and R. G. Barrera, Braz. J. Phys. **24**, 330 (1994).
[18] J. Bonča and S. A. Trugman, Phys. Rev. Lett. **75**, 2566 (1995).
[19] N. Mingo and K. Makoshi, Phys. Rev. Lett. **84**, 3694 (2000).
[20] H. Ness and A. J. Fisher, Phys. Rev. Lett. **83**, 452 (1999).
[21] E. G. Emberly and G. Kirczenow, Phys. Rev. B **61**, 5740 (2000).
[22] L. E. F. Foa Torres, H. M. Pastawski, and S. S. Makler, Phys. Rev. B **64**, 193304 (2001).
[23] N. Mingo, Liu Yang, Jie Han, and M. P. Anantram, Phys. Status Solidi B **226**, 79 (2001).
[24] D. Porezag *et al.*, Phys. Rev. B **51**, 12 947 (1995).
[25] From the point of view of momentum conservation, this process can be seen as an umklapp process.